Research Article | Vol. 25, No. 5 | 6 Mar 2017 | OPTICS EXPRESS 5457

Optics EXPRESS

Anderson localisation and optical-event horizons in rogue-soliton generation

MOHAMMED F. SALEH,[1,2,*] CLAUDIO CONTI,[3] AND FABIO BIANCALANA[1]

[1]*Scottish Universities Physics Alliance (SUPA), Institute of Photonics and Quantum Sciences, Heriot-Watt University, EH14 4AS Edinburgh, UK*
[2]*Department of Mathematics and Engineering Physics, Alexandria University, Alexandria, Egypt*
[3]*Department of Physics, University Sapienza, Piazzale Aldo Moro 2, 00185 Rome, Italy*
[4]*Institute for Complex Systems (ISC-CNR), Via dei Taurini 19, 00185 Rome, Italy*
[*]*m.saleh@hw.ac.uk*

Abstract: We unveil the relation between the linear Anderson localisation process and nonlinear modulation instability. Anderson localised modes are formed in certain temporal intervals due to the random background noise. Such localised modes seed the formation of solitary waves that will appear during the modulation instability process at those preferred intervals. Afterwards, optical-event horizon effects between dispersive waves and solitons produce an artificial collective acceleration that favours the collision of solitons, which could eventually lead to a rogue-soliton generation.

OCIS codes: (190.5530) Pulse propagation and temporal solitons; (190.4370) Nonlinear optics, fibers.

References and links

1. S. Coen, A. H. L. Chau, R. Leonhardt, J. D. Harvey, J. C. Knight, W. J. Wadsworth, and P. S. J. Russell, "White-light supercontinuum generation with 60-ps pump pulses in a photonic crystal fiber," Opt. Lett. **26**, 1356–1358 (2001).
2. L. Provino, J. M. Dudley, H. Maillotte, N. Grossard, R. S. Windeler, and B. J. Eggleton, "Compact broadband continuum source based on microchip laser pumped microstructured fibre," Electron. Lett. **37**, 558–560 (2001).
3. A. V. Avdokhin, S. V. Popov, and J. R. Taylor, "Continuous-wave, high-power, raman continuum generation in holey fibers," Opt. Lett. **28**, 1353–1355 (2003).
4. T. Schreiber, J. Limpert, H. Zellmer, A. TÃijnnermann, and K. Hansen, "High average power supercontinuum generation in photonic crystal fibers," Opt. Commun. **228**, 71 – 78 (2003).
5. W. J. Wadsworth, N. Joly, J. C. Knight, T. A. Birks, F. Biancalana, and P. S. J. Russell, "Supercontinuum and four-wave mixing with q-switched pulses in endlessly single-mode photonic crystal fibres," Opt. Express **12**, 299–309 (2004).
6. F. Vanholsbeeck, S. Martin-Lopez, M. González-Herráez, and S. Coen, "The role of pump incoherence in continuous-wave supercontinuum generation," Opt. Express **13**, 6615–6625 (2005).
7. M. H. Frosz, O. Bang, and A. Bjarklev, "Soliton collision and raman gain regimes in continuous-wave pumped supercontinuum generation," Opt. Express **14**, 9391–9407 (2006).
8. J. M. Dudley, G. Genty, and S. Coen, "Supercontinuum generation in photonic crystal fiber," Rev. Mod. Phys. **78**, 1135–1184 (2006).
9. N. R. Newbury, B. R. Washburn, K. L. Corwin, and R. S. Windeler, "Noise amplification during supercontinuum generation in microstructure fiber," Opt. Lett. **28**, 944–946 (2003).
10. S. M. Kobtsev and S. V. Smirnov, "Coherent properties of super-continuum containing clearly defined solitons," Opt. Express **14**, 3968–3980 (2006).
11. A. Demircan and U. Bandelow, "Analysis of the interplay between soliton fission and modulation instability in supercontinuum generation," Appl. Phys. B **86**, 31–39 (2006).
12. D. Tuürke, S. Pricking, A. Husakou, J. Teipel, J. Herrmann, and H. Giessen, "Coherence of subsequent supercontinuum pulses generated in tapered fibers in the femtosecond regime," Opt. Express **15**, 2732–2741 (2007).
13. D. R. Solli, C. Ropers, P. Koonath, and B. Jalali, "Optical rogue waves," Nature **450**, 1054–1057 (2007).
14. J. M. Dudley, G. Genty, and B. J. Eggleton, "Harnessing and control of optical rogue waves in supercontinuum generation," Opt. Express **16**, 3644–3651 (2008).
15. G. Genty, C. de Sterke, O. Bang, F. Dias, N. Akhmediev, and J. Dudley, "Collisions and turbulence in optical rogue wave formation," Phys. Lett. A **374**, 989 – 996 (2010).
16. R. Driben and I. Babushkin, "Accelerated rogue waves generated by soliton fusion at the advanced stage of supercontinuum formation in photonic-crystal fibers," Opt. Lett. **37**, 5157–5159 (2012).

#284789 https://doi.org/10.1364/OE.25.005457
Journal © 2017 Received 13 Jan 2017; revised 22 Feb 2017; accepted 22 Feb 2017; published 28 Feb 2017

Optics EXPRESS

17. P. T. S. DeVore, D. R. Solli, D. Borlaug, C. Ropers, and B. Jalali, "Rogue events and noise shaping in nonlinear silicon photonics," J. Opt. **15**, 064001 (2013).
18. J. M. Dudley, F. Dias, M. Erkintalo, and G. Genty, "Instabilities, breathers and rogue waves in optics," Nat. Photon. **8**, 755–764 (2014).
19. A. Armaroli, C. Conti, and F. Biancalana, "Rogue solitons in optical fibers: a dynamical process in a complex energy landscape?" Optica **2**, 497–504 (2015).
20. J. M. Soto-Crespo, N. Devine, and N. Akhmediev, "Integrable turbulence and rogue waves: Breathers or solitons?" Phys. Rev. Lett. **116**, 103901 (2016).
21. C. Kharif and E. Pelinovsky, "Physical mechanisms of the rogue wave phenomenon," Europ. J. Mechan. B Fluids **22**, 603 – 634 (2003).
22. A. R. Osborne, *Nonlinear Ocean Waves and the Inverse Scattering Transform* (Academic Press, 2010).
23. E. M. Dianov, A. Ya. Karasik, P. V. Mamyshev, A. M. Prokhorov, V. N. Serkin, M. F. Stel'makh, and A. A. Fomichev, "Stimulated-raman conversion of multisoliton pulses in quartz optical fibers," JETP Lett. **41**, 294–297 (1985).
24. F. M. Mitschke and L. F. Mollenauer, "Discovery of the soliton self-frequency shift," Opt. Lett. **11**, 659–661 (1986).
25. P. W. Anderson, "Absence of diffusion in certain random lattices," Phys. Rev. **109**, 1492–1505 (1958).
26. H. De Raedt, A. Lagendijk, and P. de Vries, "Transverse localization of light," Phys. Rev. Lett. **62**, 47–50 (1989).
27. T. Schwartz, G. Bartal, S. Fishman, and M. Segev, "Transport and anderson localization in disordered two-dimensional photonic lattices," Nature **446**, 52–55 (2007).
28. Y. Lahini, A. Avidan, F. Pozzi, M. Sorel, R. Morandotti, D. N. Christodoulides, and Y. Silberberg, "Anderson localization and nonlinearity in one-dimensional disordered photonic lattices," Phys. Rev. Lett. **100**, 013906 (2008).
29. Y. Lahini, R. Pugatch, F. Pozzi, M. Sorel, R. Morandotti, N. Davidson, and Y. Silberberg, "Observation of a localization transition in quasiperiodic photonic lattices," Phys. Rev. Lett. **103**, 013901 (2009).
30. A. Szameit, Y. V. Kartashov, P. Zeil, F. Dreisow, M. Heinrich, R. Keil, S. Nolte, A. Tünnermann, V. Vysloukh, and L. Torner, "Wave localization at the boundary of disordered photonic lattices," Opt. Lett. **35**, 1172–1174 (2010).
31. L. Levi, M. Rechtsman, B. Freedman, T. Schwartz, O. Manela, and M. Segev, "Disorder-enhanced transport in photonic quasicrystals," Science **332**, 1541–1544 (2011).
32. M. Segev, Y. Silberberg, and D. N. Christodoulides, "Anderson localization of light," Nat. Photon. **7**, 197–204 (2013).
33. M. Leonetti, S. Karbasi, A. Mafi, and C. Conti, "Observation of migrating transverse anderson localizations of light in nonlocal media," Phys. Rev. Lett. **112**, 193902 (2014).
34. M. Leonetti, S. Karbasi, A. Mafi, and C. Conti, "Light focusing in the anderson regime," Nat. Commun. **5**, 4534 (2014).
35. A. M. Jayannavar and N. Kumar, "Nondiffusive quantum transport in a dynamically disordered medium," Phys. Rev. Lett. **48**, 553–556 (1982).
36. L. Golubović, S. Feng, and F.-A. Zeng, "Classical and quantum superdiffusion in a time-dependent random potential," Phys. Rev. Lett. **67**, 2115–2118 (1991).
37. M. N. Rosenbluth, "Comment on "classical and quantum superdiffusion in a time-dependent random potential"," Phys. Rev. Lett. **69**, 1831 (1992).
38. E. Arvedson, M. Wilkinson, B. Mehlig, and K. Nakamura, "Staggered ladder spectra," Phys. Rev. Lett. **96**, 030601 (2006).
39. L. Levi, Y. Krivolapov, S. Fishman, and M. Segev, "Hyper-transport of light and stochastic acceleration by evolving disorder," Nat. Phys. **8**, 912–917 (2012).
40. G. Kopidakis and S. Aubry, "Discrete breathers and delocalization in nonlinear disordered systems," Phys. Rev. Lett. **84**, 3236–3239 (2000).
41. A. S. Pikovsky and D. L. Shepelyansky, "Destruction of anderson localization by a weak nonlinearity," Phys. Rev. Lett. **100**, 094101 (2008).
42. C. Conti and A. Fratalocchi, "Dynamic light diffusion, three-dimensional anderson localization and lasing in inverted opals," Nat. Phys. **4**, 794–798 (2008).
43. S. Flach, D. O. Krimer, and C. Skokos, "Universal spreading of wave packets in disordered nonlinear systems," Phys. Rev. Lett. **102**, 024101 (2009).
44. S. Fishman, Y. Krivolapov, and A. Soffer, "The nonlinear schrÃűdinger equation with a random potential: results and puzzles," Nonlinearity **25**, R53 (2012).
45. C. Conti, "Solitonization of the anderson localization," Phys. Rev. A **86**, 061801 (2012).
46. R. G. S. El-Dardiry, S. Faez, and A. Lagendijk, "Snapshots of anderson localization beyond the ensemble average," Phys. Rev. B **86**, 125132 (2012).
47. M. Leonetti, S. Karbasi, A. Mafi, and C. Conti, "Experimental observation of disorder induced self-focusing in optical fibers," Appl. Phys. Lett. **105**, 171102 (2014).
48. G. P. Agrawal, *Nonlinear Fiber Optics*, 4th ed. (Academic Press, 2007).
49. I. M. Lifshitz, S. A. Gredeskul, and L. A. Pastur, *Introduction to the Theory of Disordered Systems* (Wiley, 1988).
50. M. F. Limonov and R. M. De La Rue, *Optical Properties of Photonic Structures: Interplay of Order and Disorder*,(CRC, 2012).
51. P. W. Anderson, D. J. Thouless, E. Abrahams, and D. S. Fisher, "New method for a scaling theory of localization," Phys. Rev. B **22**, 3519–3526 (1980).

Optics EXPRESS

52. L. I. Deych, A. A. Lisyansky, and B. L. Altshuler, "Single parameter scaling in one-dimensional localization revisited," Phys. Rev. Lett. **84**, 2678–2681 (2000).
53. M. F. Saleh and F. Biancalana, "Soliton-radiation trapping in gas-filled photonic crystal fibers," Phys. Rev. A **87**, 043807 (2013).
54. T. G. Philbin, C. Kuklewicz, S. Robertson, S. Hill, F. König, and U. Leonhardt, "Fiber-optical analog of the event horizon," Science **319**, 1367–1370 (2008).
55. S. F. Wang, A. Mussot, M. Conforti, A. Bendahmane, X. L. Zeng, and A. Kudlinski, "Optical event horizons from the collision of a soliton and its own dispersive wave," Phys. Rev. A **92**, 023837 (2015).
56. A. Demircan, S. Amiranashvili, C. Brée, and G. Steinmeyer, "Compressible octave spanning supercontinuum generation by two-pulse collisions," Phys. Rev. Lett. **110**, 233901 (2013).
57. A. Demircan, S. Amiranashvili, C. Brée, U. Morgner, and G. Steinmeyer, "Supercontinuum generation by multiple scatterings at a group velocity horizon," Opt. Express **22**, 3866–3879 (2014).
58. A. V. Yulin, R. Driben, B. A. Malomed, and D. V. Skryabin, "Soliton interaction mediated by cascaded four wave mixing with dispersive waves," Opt. Express **21**, 14481–14486 (2013).
59. I. Oreshnikov, R. Driben, and A. V. Yulin, "Weak and strong interactions between dark solitons and dispersive waves," Opt. Lett. **40**, 4871–4874 (2015).
60. A. Demircan, S. Amiranashvili, and G. Steinmeyer, "Controlling light by light with an optical event horizon," Phys. Rev. Lett. **106**, 163901 (2011).
61. A. Demircan, S. Amiranashvili, C. Brée, C. Mahnke, F. Mitschke, and G. Steinmeyer, "Rogue events in the group velocity horizon," Sci. Rep. **2**, 850 (2012).
62. S. Pickartz, U. Bandelow, and S. Amiranashvili, "Adiabatic theory of solitons fed by dispersive waves," Phys. Rev. A **94**, 033811 (2016).
63. S. Pickartz, U. Bandelow, and S. Amiranashvili, "Efficient all-optical control of solitons," Opt. Quantum Electron. **48**, 503 (2016).

1. Introduction

Modulation instability (MI) is one of the most basic and important nonlinear optical processes. In optical fibers, MI induces spectral sidebands to narrowband optical pulses, eventually leading to a broad supercontinuum after a short propagation distance [1–7]. Generation of supercontinua via long pulses, lacks coherence and stability in comparison to using ultrashort pulses, mainly because of the amplification of the background noise [8]. Nevertheless, the understanding of the influence of the input noise on the output spectrum has driven multiple studies [9–12]. The evidence presented by Solli *et al.* that the output spectra contain statistically rare rogue events with large intensities and enhanced redshift has boosted huge research [13–20], because of the interesting connections between this phenomenon with the rare destructive rogue-waves in oceans [21, 22]. In optical rogue events, the interplay between nonlinearity and dispersion amplifies the background noise that leads to pulse break-up. Because of the Raman nonlinearity, solitons are continuously redshifted and decelerate in the time domain [23, 24]. Depending on the initial input noise, a rogue soliton with very large intensity may appear inside the fibre after multiple soliton-soliton collisions.

In this article, we present new groundbreaking details on the dynamics that proceed the collision of solitons inside of optical fibres. In particular, we describe two different processes: solitonisation of Anderson localisation (AL), followed by optical-event-horizon (OEH) induced self-frequency redshift (or deceleration in the time domain). The first process is the key element in generating solitons from the background noise during MI, whereas the collision of different solitons is facilitated by the second process. The reported concepts will be definitely important for a variety of other related fields, governed by similar models, such as ocean-wave physics, and Bose-Einstein Condensates.

In 1958 Philip Anderson reported that disorder can induce linear localised states in solid crystals, due to the cumulative effects of multiple scatterings [25]. In optics, disorder-induced transverse localisation has been demonstrated in mm-long photonic lattices [26–34]. Ensembling over multiple realisations of disorder was needed, since the propagation distance is too short to provide self-averaging. An important condition for AL to exist is to maintain the disorder along the direction of propagation. The influence of having a fluctuating disorder could re-

Optics EXPRESS

sult in superdiffussion of the optical beam, known as a hyper-transport effect [35–39]. Multiple counter-intuitive phenomena have also been reported due to the interplay between nonlinearity and AL [27, 40–47], yet a robust picture of this complex interaction is still under quest. Here, we show how a nonlinear-induced temporal potential that is disordered and slowly-evolving (quasi-static) leads to soliton formation during the MI process.

2. Anderson localisation and modulation instability

2.1. Generalised nonlinear Schrödinger equation

Using the slowly-varying envelope approximation (SVEA), the propagation of intense pulses in optical fibres can be described in terms of the generalised nonlinear Schrödinger equation (NLSE) [48],

$$\left[i\partial_z + \sum_{m\geq 2} \frac{\beta_m (i\partial_t)^m}{m!} + \gamma \left(1 + i\tau_{sh}\partial_t\right) \left(R(t) \otimes |A|^2 \right) \right] A = 0, \tag{1}$$

where $A(z,t)$ is the pulse complex envelope, z is the propagation direction, t is the time-delay in a reference frame moving with the pulse group velocity, β_m, γ, τ_{sh} are the dispersion, nonlinear and self-steepening coefficients, respectively, $R(t)$ is the nonlinear response function that includes Kerr and Raman contributions, $\otimes$ denotes the convolution integral, $\gamma = n_2\omega_0/cA_{\text{eff}}$, n_2 is the nonlinear refractive in units of m^2/W, ω_0 is the pulse central frequency, c is the speed of light in vacuum, and A_{eff} is the effective optical mode area. Neglecting higher-order nonlinear and dispersion coefficients, Eq. (1) can be written as

$$i\partial_z A - \frac{\beta_2}{2}\partial_t^2 A + \frac{\omega_0}{c}\Delta n(z,t)A = 0, \tag{2}$$

where the nonlinear-Kerr term results in a pure spatio-temporal modulation of the refractive index $\Delta n(z,t) = n_2|A|^2/A_{\text{eff}}$, which will follow the variation of the pulse intensity during propagation in z. In the anomalous dispersion regime, the amplification of the background noise after a short propagation distance is inevitable for long pulses, resulting in a random temporal modulation of the refractive index.

2.2. Linear localised Anderson modes in temporal potentials

The random temporal modulation of the refractive index induced by strong long pulses during the propagation inside optical fibres corresponds to an optical potential $U = \omega_0\Delta n/c$ with allowed linear modes, which will follow the track of the pulse. These modes are the solutions of the following linear Schrödinger equation,

$$i\partial_z u_k - \frac{\beta_2}{2}\partial_t^2 u_k + U(z,t)u_k = 0, \tag{3}$$

where u_k is the complex amplitude of the mode $k = 0, 1, 2, \ldots$ Expressing $u_k(z,t) = f_k(t)\exp(i\lambda_k z)$, Eq. (3) becomes an eigenvalue problem with f_k and λ_k representing the eigenfunctions and eigenvalues, respectively. The SVEA implies that $|\partial_z\Delta n| \ll \omega_0 |\Delta n|/c$, therefore, $\Delta n(z,t) \approx \Delta n(t)$ is frozen over short spatial z-intervals. In other words, Eq. (3) becomes the 1-D temporal analogue of the transverse-disorder Anderson waveguides, where linear temporal Anderson localised states could be formed. Optical fibres are usually meters long and the complex envelope varies slowly over tenth of centimetres or even meters (i.e. 1 – 2 orders of magnitude longer than the waveguides used in AL experiments [26–34]). Therefore, temporal Anderson localisation could be realised in optical fibres for any input-noise profile. The localisation is due to the interference between forward and backward waves in the time domain of the moving reference frame that allows positive and negative delays without violating causality.

Optics EXPRESS

The localisation time $T_{\mathrm{loc}}^{(k)}$ of a linear mode k is given by [45, 49],

$$T_{\mathrm{loc}}^{(k)}(z) = \frac{\left(\int |f_k(z,t)|^2\, dt\right)^2}{\int |f_k(z,t)|^4\, dt}. \tag{4}$$

For the ground state, $T_{\mathrm{loc}}^{(0)}(z)$ is the inverse of the Lyapunov exponent Γ that is a self-averaging quantity [50]. Γ satisfies the single parameter scaling equation [51, 52], which in 1-D random temporal scheme is given by $\Delta^2 = \Gamma/T_0$, where Δ^2 is the variance of Γ and T_0 is the input pulse width. We have maintained the spatial dependence of $T_{\mathrm{loc}}^{(k)}$ and Γ to determine the effect of the evolution of the potential on these quantities.

2.3. Solitonisation of Anderson localisation

Consider the propagation of a long superGaussian pulse with central wavelength 1060 nm, full-width-half-maximum (FWHM) 7 ps, and input power 100 W in a solid silica-core photonic crystal fibre with zero-dispersion wavelength located at 1055 nm. The coefficients of dispersion, Kerr nonlinearity and self-steepening follow Ref. [14]. A superGaussian pulse induces a temporal quasi step-index rectangular waveguide. To understand the role of the noise, we first simulate Eqs. (2)–(3). Figure 1(a) show the temporal evolution of the nonlinear pulse. Starting from $z = 0$, the background noise builds up and then alters the pulse amplitude around $z \approx 5.5$ m due to MI. In panel (b), it depicts how the associated linear fundamental mode is adiabatically compressed significantly due to AL until $z \approx 5.5$ m. The temporal position of localisation is completely random, and it relies on the shape of the input noise. Since the temporal-induced potential is evolving, the localisation process is halted at that position, and the fundamental mode attempts to sustain at other places for few centimetres. Discretising the optical fibre into small segments after MI occurs, one could regard each segment as a different random system, where AL attempts to occur. As a posteriori justification of our assumption of having 'quasi-static' random temporal potential, we have plotted in panel (c) the normalised quantity $L_{\mathrm{NL}}\, \partial_z \tilde{\sigma}^2$, where $\tilde{\sigma}^2 = \sigma^2/\sigma^2(0)$, σ^2 is the variance of the potential U, and L_{NL} is the nonlinear length [48]. Clearly, the potential varies very slightly in comparison to its initial value.

The characteristics of the fundamental Anderson mode measured by its localisation time and eigenvalue are shown in panel (d). In the regime where AL exists, the temporal width and the eigenvalue of the ground state are significantly reduced. When AL stops, the fundamental mode starts to jump from one potential dip to another, resulting in fluctuating behaviour of its eigenvalue. In panel (e), we show the first 20 Anderson eigenmodes on the top of each other, where each mode is normalised such that its energy is unity. The characteristics of some of these modes are plotted in panel (d). The excitation of different combinations of these modes and their final temporal positions strongly depend on the input-pulse parameters and the specific noise profile.

These Anderson modes seed the emission of solitons shown in Fig. 1(a), a phenomenon known as solitonisation of Anderson localisation [45]. In other words, when the linear modes become intense enough, they start to form solitons in the presence of the right sign of second-order dispersion. These types of seeded solitons, include Akhmediev breathers (AB) and Kuznetsov-Ma (KM) solitons [18], displayed in the insets of Fig. 1(a), generally exhibit periodicity in both time and longitudinal direction. Solitons are emitted with close amplitudes around $z \approx 5.5$ m, because their corresponding modes have close eigenvalues that play the role of the free parameter in the breather solution of the NLSE [18]. However, in the presence of higher-order perturbations in the NLSE, the solution becomes a perturbed fundamental soliton (sech-pulse), which will be similarly seeded by the Anderson modes as discussed below. We would like to

Optics EXPRESS

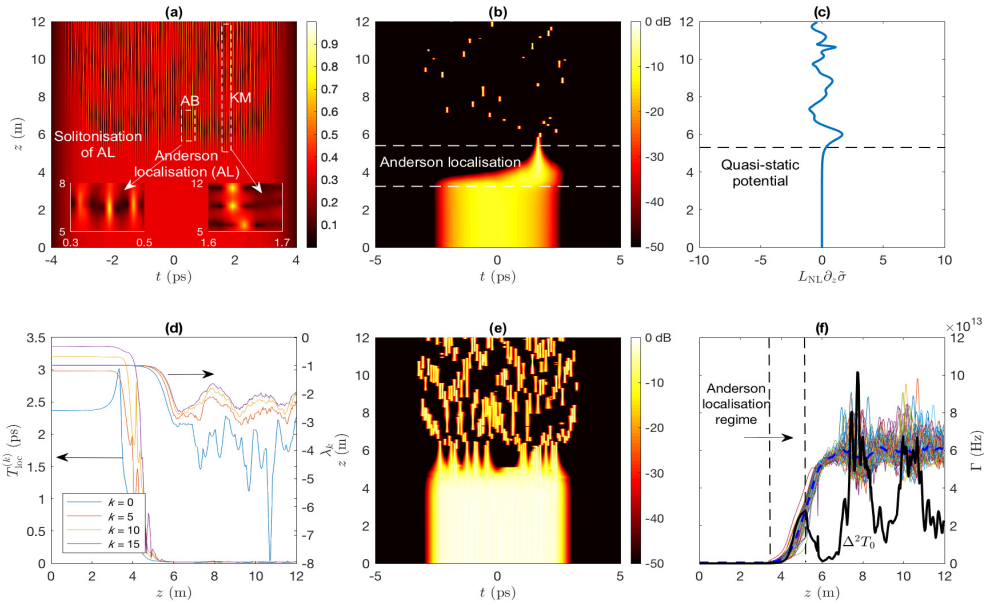

Fig. 1. (a) Temporal evolution of a superGaussian pulse $A = \exp\left[-1/2\,(t/T_0)^{10}\right]$ at wavelength 1060 nm, with $T_0 = 3.63$ ps (FWHM = 7 ps) and input power 100 W inside the solid silica-core photonic crystal fibre of Ref. [14] in the absence of higher-order dispersion, Raman effect and self-steepening. (b) Temporal evolution of the ground Anderson state of the induced temporal-waveguide. (c) Spatial dependence of the quantity $L_{\rm NL}\,\partial_z\tilde{\sigma}^2$. (d) Spatial evolution of the localisation times and eigenvalues of four Anderson modes with $k = 0, 5, 10, 15$. (e) Temporal evolution of the amplitude of the first 20 linear modes on the top of each other. Each mode is normalised such that its energy is unity. (f) Spatial dependency of the Lyapunov exponent Γ, its mean (dashed blue), and variance (solid black) of an ensemble of 50 different input shot noise.

emphasise that this is different from the traditional case where a regular soliton is always associated with two trapped even and odd modes due to the fixed relation between the soliton amplitude and width [53].

We also studied the dependence of the localisation time of the fundamental mode on the input shot noise. The spatial dependency of Γ, its mean, and variance Δ^2 of an ensemble of 50 simulations of different random shot noise are depicted in panel (f). Until $z = 6$ m, Γ or $T_{\rm loc}^{(0)}$ is almost independent of the noise input profile. Moreover, Γ and $\Delta^2\,T_0$ initially follow the single parameter scaling equation until $z \approx 5.5$ m, where our quasi-static approximation starts to break down, see panel (c). The non-vanishing variance in this regime shows that the temporal position of the fundamental mode depends on the input-noise profile.

3. Optical-event horizons

As illustrated in the previous section, solitons are generated after MI with close amplitudes, hence, they are anticipated to follow parallel trajectories that disfavour soliton collisions in the presence of Raman nonlinearity. Beside AL, optical-event horizons (OEHs) [54] are also playing a major role in rogue-soliton generation that is mainly based on collision of solitons. The nonlinear temporal waveguide due to a strong pump pulse in a Kerr medium acts as an optical barrier such that a trailing probe pulse with slightly higher group velocity cannot penetrate

Optics EXPRESS

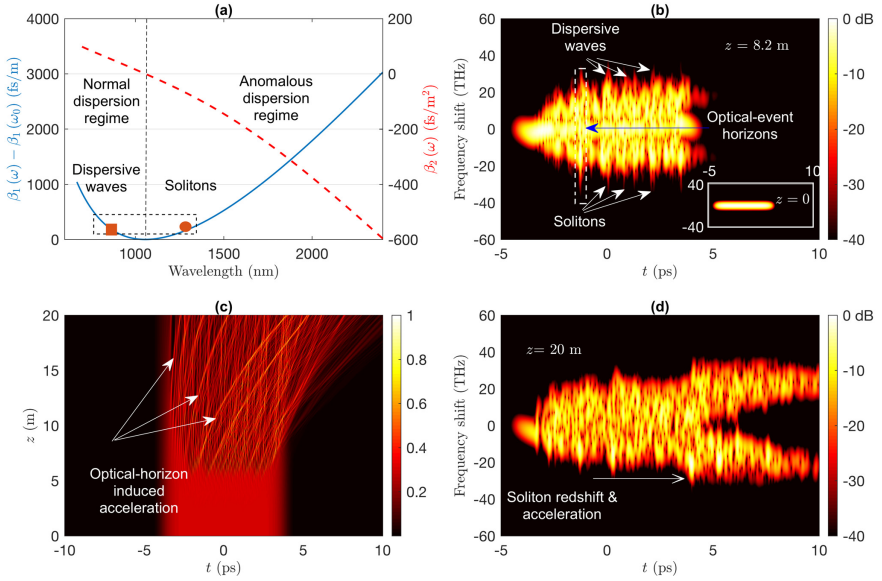

Fig. 2. (a) Wavelength-dependence of first-order β_1 and second-order β_2 dispersion coefficients. The dotted rectangle shows a group of a soliton and a dispersive-wave with nearly group velocities. (b) XFROG representation of the superGaussian pulse at $z = 8.2$ m. The inset is XFROG at $z = 0$. (c) Temporal evolution of the superGaussian pulse. (d) XFROG representation of the superGaussian pulse at $z = 20$ m. Simulations in this figure are performed using Eqs. (1) and (3) in the absence of $\beta_{m\geq 4}$, τ_{sh}, and Raman nonlinearity.

and bounces back [54, 55]. Because of the cross-phase modulation the probe speed slows down until it matches the strong pulse velocity, so the two pulses are locked together and nonlinearly interact for a long distance. This phenomenon has also been predicted for probe powers and energies closer or even greater than the pump [56]. Exploiting this effect, octave-spanning highly-coherent supercontinua [56, 57], and soliton interactions mediated by trapped dispersive waves [58, 59] can be attained. Rogue events in the group-velocity horizon due to soliton and dispersive waves interactions have been also considered [60, 61].

Adding the third-order dispersion in Eq. (2) will force solitons to emit and trap dispersive waves that are seeded by the background noise, due to satisfying the phase matching conditions. A large pool of solitons and dispersive waves will form via MI. Near the zero dispersion wavelength, the concave group-velocity β_1 dispersion, as shown in Fig. 2(a), enables synchronous co-propagation of solitons and dispersive waves in the anomalous and normal dispersive regimes, respectively. Hence, the condition for the optical group-velocity event horizon [54] between a leading soliton and a trailing dispersive wave can be easily met. This is evident in the cross frequency optical gating spectrogram (XFROG) at $z = 8.2$ m in Fig. 2(b). In this case, the soliton-induced potential barrier impedes the flowing of the dispersive wave and reflect it back after collision. Interestingly, the collision can result in a soliton self-frequency redshift accompanied by a deceleration in the time domain even in the absence of Raman nonlinearity, as depicted in Figs. 2(c)–2(d) that present the temporal evolution of the pulse inside the fibre and the XFROG at $z = 20$ m. This deceleration is stronger for solitons at the leading edge, since they are trailed by a large number dispersive waves. Analytical description of this type of acceleration for a single collision between a soliton and a dispersive wave has been the subject of a very recent work [62, 63]. The opposite scenario with a trailing soliton colliding with a dispersive wave at

Optics EXPRESS

slightly different velocity has been exploited for obtaining soliton blueshift [56, 57].

The third-order dispersion enhances the evolution of the background noise starting from $z \approx 6$ m, after AL takes place. We have found that the inclusion of higher-order dispersion coefficients $\beta_{m>3}$ and self-steepening effects τ_{sh} does not involve additional features in pulse dynamics, other than fostering the randomness of the temporal potential.

4. Soliton clustering and rogue-soliton generation

In this section, we will apply our findings of AL and OEHs in elaborating how a rogue soliton is generated. Figures 3(a)–3(b) displays the spectral and temporal evolution of the superGaussian pulse with Raman effect producing strong soliton self-frequency redshift and deceleration in the time domain. Simulations in Fig. 3 are performed by solving Eqs. (1) and (3), i.e. including Kerr, Raman, self-steepening, and higher-order dispersion coefficients until the tenth-order. Due to AL, the quasi-static induced random potential allow localised modes to exist, which in turn seed the emission of solitary waves as shown in panel (c). This plot shows the track of the first 20 Anderson modes, which are usually very sufficient to describe the key players in rogue-soliton generation. The tracks of these modes will experience discontinuities with any slight perturbation, because they have close eigenvalues. The dependence of the Lyapunov exponent Γ, its mean, and variance on the input shot noise is presented in panel (d), anticipating the regime where AL takes place. In comparison to the ideal case presented in 1(f), the length of this regime has been reduced by ≈ 0.5 m long due to the inclusion of higher-order perturbation terms in the NLSE.

Soliton collisions occur when their trajectories intersect, however, specific scenarios lead to rogue solitons with large amplitude and frequency redshift. Raman nonlinearity induces soliton acceleration that is proportional to the quartic of its amplitude. Hence, soliton collisions are unlikely to initially occur, since solitons will follow nearly parallel trajectories. However, because of OEH-induced acceleration due to solitary and dispersive waves collisions, soliton trajectories start to intersect. Raman nonlinearity allows the solitons to cluster in the time and frequency domains very quickly, as depicted in the XFROG representation in Figs. 3(e)–3(f). This results in strong temporal overlap and close group velocities for the solitons, so they could strongly nonlinearly interact for a long distance and a rogue-soliton is generated after exchanging energy between them, as shown in Figs. 3(b) and 3(f). This cluster of solitons is analogous to an OEH made of different pulses, however, with similar amplitudes.

The statistics of a rogue-soliton emission that follows the L-shaped Weibull distribution depends mainly on the intense of soliton-soliton collisions and the fibre length. In the case of pumping near the zero-dispersion wavelength, soliton collisions are nearly inevitable due to OEH-induced acceleration that changes the soliton paths. We have found only around 50 events, where solitons could have parallel trajectories inside a fibre of 20 m long, from an ensemble of 1000 different input noise. This number is also significantly dropped if the fibre length is increased. The intensity of a rogue-soliton is based on how many clusters are formed, how many solitons are within each cluster, and how these solitons are temporally overlapped.

5. Conclusions

We have reported the missing ingredients of the generation of a rogue-soliton in optical fibres. We have found that the true origin of soliton generation during the modulation instability process stems from the temporal Anderson localisation effect. Solitary-waves that appear from nowhere during propagation of a nonlinear pulse inside an optical fibre are seeded by the linear eigenmodes of a 1-D temporal Anderson crystal. The usual pumping near the zero-dispersion-wavelength for obtaining broadband supercontinua favours optical-event horizons formation between solitons and dispersive waves. The latter effect results in an additional soliton acceleration, besides the usual Raman-induced one. This acceleration is unbalanced towards the pulse

Optics EXPRESS

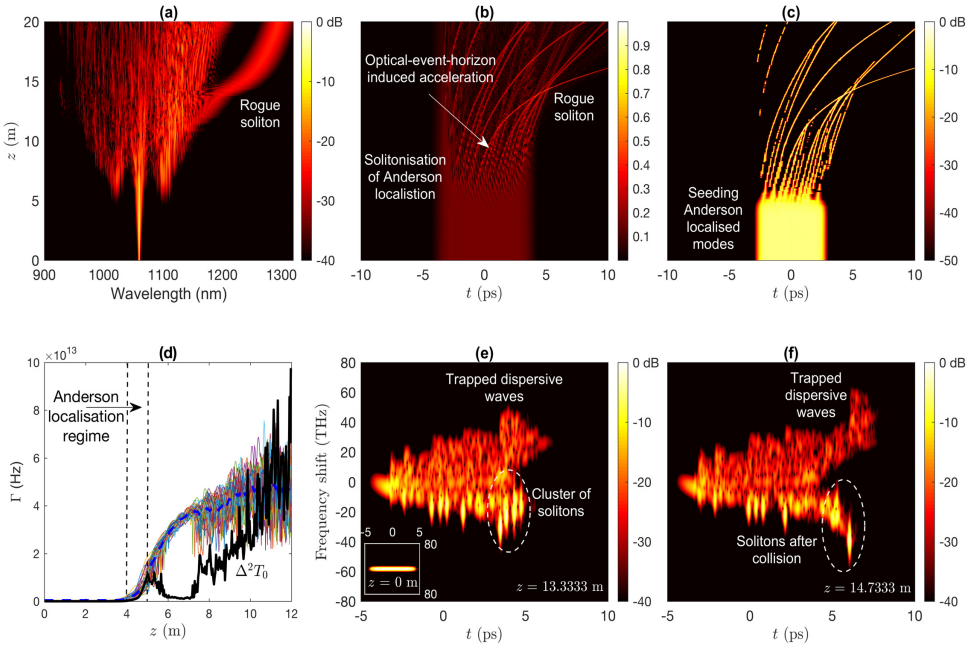

Fig. 3. (a,b) Spectral and temporal evolution of the superGaussian pulse. The temporal contour plot is normalised to its peak. (c) Temporal evolution of the first 20 Anderson eigenmodes. (d) Spatial dependency of the Lyapunov exponent Γ, its mean (dashed blue), and variance (solid black) of an ensemble of 50 different input shot noise. (e,f) XFROG representation of the superGaussian pulse inside the fibre at z =13.3 m and 14.73 m. The inset in (e) is XFROG at $z = 0$. Simulations in this figure are performed using the full Eqs. (1) and (3).

leading edge and favours soliton-soliton collisions. Rogue solitons are generated after strong temporal overlap between individual solitons with close group velocities, due to Raman nonlinearity.

We believe that our findings solve one of the most debated questions in the field, namely: are rogue waves generated by processes that are intrinsically linear or nonlinear? The answer to this question is that a linear process, Anderson localisation, seeds temporal localised structures from the background noise. Subsequently a nonlinear phenomenon, the solitonisation of Anderson localisation, together with optical-event horizons induce the last steps of rogue-soliton formation.

These rich mechanisms demonstrate the complexity underlying rogue-soliton generation and furnish a clear evidence of the previously-unconsidered temporal Anderson localisation, and the unexpected interaction with optical-event horizons. This scenario will potentially lead to novel routes for controlling of extreme nonlinear waves via linear-disorder optimisation.

Funding

Royal Society of Edinburgh (RSE) (501100000332).